# Characterization of Alkyl Chain Conformation in an Intercalated Cationic Lipid Bilayer by IR Spectroscopy

**N. V. Venkataraman and S. Vasudevan***

*Department of Inorganic and Physical Chemistry, Indian Institute of Science, Bangalore 560 012, India*

*Received: March 9, 2002; In Final Form: April 30, 2002*

A structural analysis of alkyl chain conformation of an intercalated cationic lipid bilayer is described. Dialkyl dimethylammonium ions (*di*-$C_n$DA) were ion exchanged into the galleries of layered cadmium thiophosphate to give $Cd_{0.83}PS_3$(*di*-$C_n$DA)$_{0.34}$. The grafting density and interlayer expansions were identical to those for the intercalated single chain alkyl trimethylammonium ($C_n$TA) bilayers. The increased methylene chain density in the galleries, however, forces the intercalated lipid to adopt a more trans ordered structure. Progression bands arising from the coupling of vibrational modes of trans methylene units are used to establish the extent of trans registry. Two types of ordered structures of the intercalated cationic lipid may be distinguished. One in which both alkyl chains adopt an all-trans geometry, and one in which the methylene bond adjacent to the headgroup on one of the alkyl chains is gauche. The latter structure is typically found in the crystalline state of these cationic lipids. The concentrations of the two structures were determined from the ratio of the intensities of the progression bands and were found to remain unchanged with temperature.

## Introduction

Studies on the structure and physical properties of lipid bilayers and lipid molecular assemblies are of fundamental importance in providing insights into the structure and organization of biomembranes.[1,2] Studies of synthetic lipids by spectroscopic techniques have played a key role in understanding the role of conformational disorder as well as in the development of techniques to characterize disorder of the acyl chains.[3−5] Among the earliest reported synthetic amphiphiles which conform membrane-like bilayer structures are the dialkyl dimethylammonium bromides[6] [$(C_nH_{2n+1})_2N^+(CH_3)_2Br^-$]. Hydrated bilayer dispersions of these cationic lipids[7,8] and their mixtures with membrane components such as cholesterol[9] and gramicidin[8] have been studied as models for the more complex biomembranes.

Intercalation of bilayer-forming cationic lipid-like surfactants in a variety of inorganic layered solids is known in the literature.[10−15] In these systems, the cationic headgroup is tethered to the internal surface of the galleries of the layered solid via coloumbic interactions. The surfactant molecules in the galleries can adopt a variety of structures—monolayer, bilayer, or paraffin-type bilayer—depending on the packing density and length of the surfactant methylene "tail". At low grafting densities, the surfactant molecule lie flat but, with increasing grafting density, usually adopt either a bilayer or interdigitated-bilayer structure. These organic−inorganic hybrid materials have been studied as crystalline, immobile models of biomembranes.[10] These materials also find use as precursors for the preparation of clay-polymer nanocomposites,[16−18] and their utility in the removal of organic contaminants in water treatment have also been recognized.[19,20]

Recently, we had reported the intercalation of the single-chain cetyl trimethylammonium (CTA) ions, [$C_{16}H_{33}N^+(CH_3)_3$], in layered cadmium thiophosphate.[21] This host lattice is formed by the stacking of $CdPS_3$ sheets built by the edge-sharing of $CdS_6$ and $P_2S_6$ polyhedra.[22,23] The surfactant ions were introduced into the galleries by an ion-exchange intercalation reaction in which charge neutrality is maintained by an equivalent loss of divalent Cd ions from the layer to form $Cd_{0.83}PS_3(CTA)_{0.34}$. Within the galleries, the intercalated surfactant molecules adopt a tilted bilayer structure. Using vibrational spectroscopy, it had been possible to establish the extent of conformational order. The confined methylene chains adopt an essentially all-trans conformation, and although the concentration of gauche conformers was small, it was possible to identify specific conformational sequences containing gauche bonds.[21] Here, we report the intercalation of the double-chain, dialkyl dimethylammonium ions (*di*-$C_n$DA) [$(C_nH_{2n+1})_2$ $N^+(CH_3)_2$] ($n$ = 16 and 18), in layered $CdPS_3$. We find the lattice expansion on intercalation and the grafting density for these cationic lipid-like surfactants to be identical to that for the intercalated single-chain surfactant ions. This system, therefore, allows us to examine the effect of increased methylene chain density in the interlamellar region on the conformation of the intercalated surfactant. Because methylene chains of the intercalated single chain surfactant CTA are fairly ordered,[21] one would expect a still greater degree of conformational order for the intercalated double-chain (*di*-$C_n$-DA) surfactant. We have used vibrational spectroscopy, mainly infrared, to probe conformational order of the intercalated lipid-like surfactants, because of the effectiveness of the technique in determining low concentrations of disorder in an ensemble of alkyl chains which are predominantly ordered in all-trans conformation.

We have also established the nature of the conformationally ordered structure of the intercalated (*di*-$C_n$DA) chains. Two types of ordered states may be distinguished, one in which both alkyl chains adopt an all-trans geometry (TT) (Figure 1a) and one in which the $CH_2-CH_2$ bond next to the headgroup on one of the alkyl chains is gauche (TG; Figure 1b). The later structure is the one found in the crystalline forms of the dialkyl dimethylammonium bromides.[24,25] The number of methylene

* To whom correspondence should be addressed. E-mail: svipc@ipc.iisc.ernet.in.

10.1021/jp025743g CCC: $22.00 
Published on Web 07/18/2002

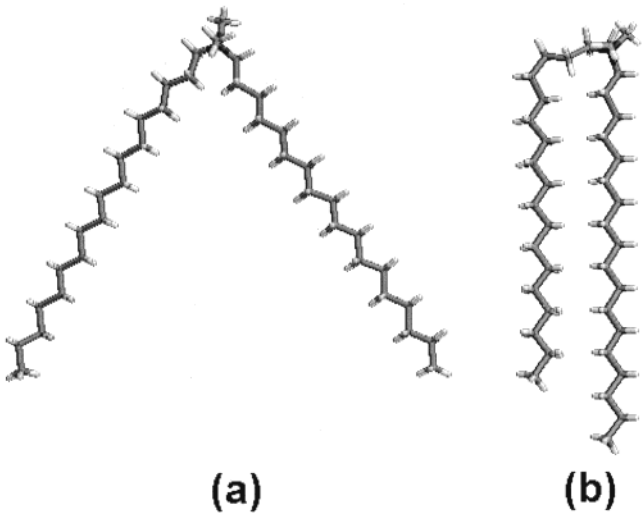


**Figure 1.** Two types of conformations adopted by dialkyl dimethylammonium cationic lipids. In part a, both of the alkyl chains are in an all-trans conformation (TT), and in part b one of the alkyl chains adopts a gauche conformation near the "head" group (TG). The later is the one found in the crystalline state of these lipids.[24,25]

units in all-trans registry is different for the two chains in the TG structure (Figure 1b), whereas for the TT (Figure 1a) structure, they are identical. This situation is very similar to that found in lipids such as the diacyl phospholipids[26] where the SN1 and SN2 chains could both be all trans (TT)[27] or either the SN1 or SN2 chains could have the methylene bond adjoining the lipid headgroup adopt a gauche conformation (TG).[26] We use the method developed by Yan et al.[27] to distinguish between these two structures and to determine their relative concentrations. The method exploits the fact that the number and spacing of the progression bands in the infrared spectrum, arising from a coupling of the wagging and rocking-twisting modes of *trans*-methylene units, depends on the number of methylene units in trans registry.

## Experimental Section

Cadmium thiophosphate, $CdPS_3$, was prepared from the elements following the procedure reported in the literature.[28] Cadmium metal powder, phosphorus, and sulfur in stoichiometric amounts were sealed in quartz ampules at $10^{-6}$ Torr and heated at 650 °C for two weeks. Single crystals of $CdPS_3$ were grown by chemical vapor transport using excess sulfur as a transporting agent. The dialkyl dimethylammonium bromides were obtained from Aldrich (97% purity) and were recrystallized from $CHCl_3$/hexane. Octadecyl trimethylammonium bromide-(ODTAB) (Aldrich, 95% purity) and cetyl trimethylammonium bromide(CTAB) (Loba Chem) were recrystallized from ethanol/diethyl ether.

Intercalation of the surfactant cations was effected by a two-step ion-exchange process. In the first step, hydrated potassium ions are ion-exchange intercalated within the galleries of $CdPS_3$, with an equivalent loss of cadmium ions from the layer and a lattice expansion of 2.8 Å:[29−31]

$$CdPS_3 + 2xK^+_{(aq)} \xrightarrow{\text{EDTA}} Cd_{1-x}PS_3K_{2x}(H_2O)_y + xCd^{2+}_{(aq)} \quad (x = 0.17)$$

In the second step, the intercalated hydrated potassium ions are exchanged for the surfactant cation:

$$Cd_{1-x}PS_3K_{2x}(H_2O)_y + 2xSA^+_{(aq)} \rightarrow Cd_{(1-x)}PS_3(SA)_{2x} + 2xK^+_{(aq)} \quad (x = 0.17)$$

where $SA^+$ are the surfactant cations, *di*-$C_nDA^+$ or the single chain $CTA^+$ or $ODTA^+$ ions. Irrespective of the surfactant cation, the exchange reaction in the second step was quantitative.

Crystals of $CdPS_3$ were treated with a 4 M aqueous solution of KCl in the presence of 0.1 M EDTA and 1 M $K_2CO_3$/$KHCO_3$ as buffer, to give $Cd_{0.83}PS_3K_{0.34}(H_2O)$. The compound has a lattice spacing of 9.4 Å, corresponding to a lattice expansion of 2.8 Å as compared to pristine host $CdPS_3$.[29−31] The interlamellar potassium ions in $Cd_{0.83}PS_3K_{0.34}(H_2O)$ were further ion-exchanged with surfactant ions. In a typical reaction $Cd_{0.83}PS_3K_{0.34}(H_2O)$ was refluxed with a 0.02 M methanol/water solution of the respective dialkyl dimethylammonium bromide at 60 °C for 6 h to give $Cd_{0.83}PS_3$(*di*-$C_nDA)_{0.34}$. Completion of ion-exchange was ascertained from the disappearance of the *00l* reflection of $Cd_{0.83}PS_3K_{0.34}(H_2O)$ in the X-ray diffraction pattern and the appearance of a new series of *00l* reflections corresponding to the formation of $Cd_{0.83}PS_3$(*di*-$C_nDA)_{0.34}$. Ion-exchange intercalation of the alkyl trimethylammonium cations ($C_nTA$: $n = 16$ and 18) were effected by a similar procedure with a 0.05 M aqueous solution of the surfactant at 50 °C giving $Cd_{0.83}PS_3(C_nTA)_{0.34}$.

Cadmium ion stoichiometry was established by atomic absorption spectroscopy (Perkin-Elmer 4381), and the organic part was established by C, H, and N analysis. Powder X-ray diffractions were recorded on a Shimadzu-XD-D1 diffractometer using Cu Kα radiation. Crystals were mounted flat on a sapphire disk, which occupied the same position as the regular sample holder on the X-ray goniometer. FT-Raman spectra were recorded on a Bruker IFS FT-Raman spectrometer, using a Nd:YAG (wavelength 1.064 $\mu$m) laser as exciting radiation. All spectra were recorded at 4 $cm^{-1}$ resolution with an unpolarized beam. Laser power was kept at 200 mW and typically ∼500 spectra were co-added to improve the signal-to-noise. Infrared spectra of crystals of were recorded in the spectral range 400−4000 $cm^{-1}$ on a Bruker IFS55 spectrometer. The crystals were mounted on a hollow copper block and cooled using a CTI−Cryogenics closed-cycle cryostat, and the sample temperature could be varied from 300 to 40 K.[32]

## Results

**(a) X-ray Diffraction.** The X-ray diffraction patterns of crystals of $CdPS_3$ intercalated with the cationic lipid, $CdPS_3$.*di*-$C_nDA$, (solid line) along with those for the corresponding single chain alkyl trimethylammonium ion intercalates $CdPS_3.C_nTA$ (dashed line) are shown in Figure 2. As mentioned in the Experimental Section, the diffraction patterns are for crystals mounted flat on a sapphire disk, and hence, only the *00l* reflections are observed. The interlayer spacings of the $CdPS_3$.*di*-$C_nDA$ as calculated from the *00l* reflections are 33.0 and 36.5 Å for $n = 16$ and 18, respectively, whereas for the single chain $CdPS_3.C_nTA$, they are 33.0 Å for $n = 16$ and 36.5 Å for $n = 18$.

For the intercalated single chain $CdPS_3.C_{16}TA$, it had been shown that within the galleries the surfactant ions adopt a tilted bilayer arrangement.[21] The tilt angle, the angle the molecular axis of the intercalated methylene chains makes with the interlayer normal, had been determined from infrared dichroic measurements to be 52°. This value is identical to that calculated for a tilted bilayer from the length of an all-trans cetyl chain

**TABLE 1: Observed Infrared and Raman Frequencies of the Intercalates $CdPS_3.C_nTA$ and $CdPS_3.di\text{-}C_nDA$ along with Their Assignments**

| infrared | | | Raman | | |
|---|---|---|---|---|---|
| $CdPS_3.di\text{-}C_nDA$ ($cm^{-1}$) | $CdPS_3.C_nTA$ ($cm^{-1}$) | assignment | $CdPS_3.di\text{-}C_nDA$ ($cm^{-1}$) | $CdPS_3.C_nTA$ ($cm^{-1}$) | assignment |
| 3012 (m) | 3014 (m) | $N^+-CH_3$ asym stretch | 3019 (w) | 3019 (m) | $N^+-CH_3$ C−H stretch |
| 2952 (m) | 2952 (sh) | $CH_3$ asym stretch | 2958 (w) | 2962 (w) | $CH_3$ asym stretch |
| 2918 (s) | 2918 (s) | $CH_2$ anti sym stretch | 2927 (w) | 2927 (w) | $CH_2$ anti sym stretch |
| 2872 (sh) | 2872 (sh) | $CH_3$ sym stretch | 2880 (s) | 2882 (s) | $CH_3$ sym stretch |
| 2848 (s) | 2850 (s) | $CH_2$ sym stretch | 2848 (s) | 2850 (s) | $CH_2$ sym stretch |
| 1465 (s) | 1465 (s) | $CH_2$ scissoring | 1460 (sh) | | $N^+-CH_3$ bend |
| 1417 (w) | 1417 (w) | | 1440 (s) | 1442 (s) | $CH_2$ scissoring |
| 1396 (w) | 1396 (w) | | 1297 (s) | 1297 (s) | $CH_2$ twisting |
| 1377 (m) | 1377 (w) | $CH_3$ sym bending | 1130 (m) | 1128 (m) | C−C skeletal stretch |
| | 964 (s) | $C-N^+$ stretch | 1064 (m) | 1064 (m) | C−C skeletal stretch |
| 910 (m) | 912 (s) | $C-N^+$ stretch | 890 (w) | | |
| 720 (s) | 720 (s) | $CH_2$ rocking | 769 (w) | 765 (w) | $C-N^+$ stretch |

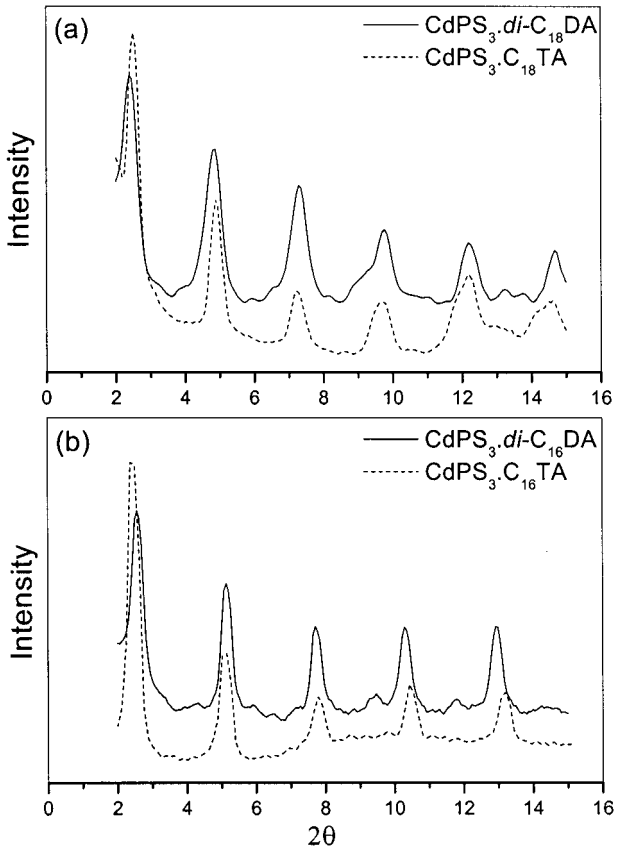


**Figure 2.** Powder X-ray diffraction patterns showing the *00l* reflections of crystals of the cationic lipid intercalates $CdPS_3.di\text{-}C_nDA$ (solid line) along with the corresponding single chain analogues $CdPS_3.C_nTA$ (dotted line) for different chain lengths **(a)** $n = 18$ and **(b)** $n = 16$.

and the observed X-ray interlayer spacing.[21] A similar calculation from the observed interlayer spacing for the single chain intercalated $CdPS_3.C_{18}TA$ give a value of 53° for the tilt angle. In view of the observed similarity in the lattice spacings and the chemical composition for the double chain $CdPS_3.di\text{-}C_nDA$ and single chain $CdPS_3.C_nTA$ intercalates, it is reasonable to assume that the intercalated double chains $di\text{-}C_nDA$, too, adopt a tilted bilayer structure in the galleries. This system, therefore, allows for a direct measure of the effect of increased density of methylene chains on conformational order.

The similar grafting densities and lattice expansions for the double chain and the corresponding single chain surfactants may at first seem surprising. It may, however, be noted that the methylene chain density in the interlamellar space of the intercalated single chain compounds ($CdPS_3.C_nTA$) is considerably lower than that of the corresponding crystalline salts. The volume available on the gallery space of the intercalated single chain compounds could have, in principle, accommodated a large concentration of surfactant molecules. The grafting density in these $CdPS_3$ intercalates is however decided, at least in part, by the extent of ion-exchange which in turn is decided by the concentration of cationic vacancies that the $CdPS_3$ lattice can support. In the ion-exchange intercalation compounds of $CdPS_3$, the observed cation vacancies are typically in the range of $0.07 < x < 0.25$.[21,31,32] It is for this reason that the double chain and single chain intercalation compounds show a similar grafting density.

**(b) Vibrational Spectroscopy.** The IR and Raman spectra of the intercalated cationic lipids $CdPS_3.di\text{-}C_nDA$ and the corresponding single chain $CdPS_3.C_nTA$ were recorded at room temperature. The observed peak positions in the IR and Raman spectra along with assignments are given in Table 1. The peak positions for the intercalated surfactant cations are almost identical to that of their crystalline bromide salts, and consequently, the assignments are similar. The assignment of the vibrational bands of the CTA ion intercalate $CdPS_3.C_{16}TA$ had been reported earlier.[21]

In the intercalated cationic lipids $CdPS_3.di\text{-}C_nDA$ and the corresponding crystalline bromides ($di\text{-}C_nDAB$), neither the methylene scissoring mode (1467 $cm^{-1}$) nor the rocking mode (720 $cm^{-1}$) are split into two components. For the corresponding single chain analogues, however, these modes are split in the crystalline state, but in the intercalate, $CdPS_3.C_nTA$, they appear as a single component. These modes are known to be sensitive to the packing arrangement in alkyl chain assemblies.[33] In an orthorhombic arrangement, these modes are split due to lateral interchain interactions between contiguous $CH_2$ groups of adjoining chains. In monoclinic and triclinic packing where there is only one chain per unit cell as well as in alkane chain assemblies of low density where lateral interchain interactions are weak, splitting of these modes is absent.

In the following sections, we look at those vibrational modes of the intercalated surfactant which are known to be sensitive to the conformation of the methylene chain.

**C−H Stretching Region.** The position, splitting and intensities of the methylene stretching modes in the infrared and Raman spectra have been extensively used in the study of conformation of alkyl chain assemblies.[34−36] The frequencies of the symmetric and antisymmetric methylene stretching modes in the IR spectrum has been used as a measure of chain conformation. For trans-ordered alkyl chains as in the crystalline *n*-alkanes, the symmetric and antisymmetric $-(CH_2)-$ stretching modes appear in the ranges of 2846−2849 and 2916−2919 $cm^{-1}$

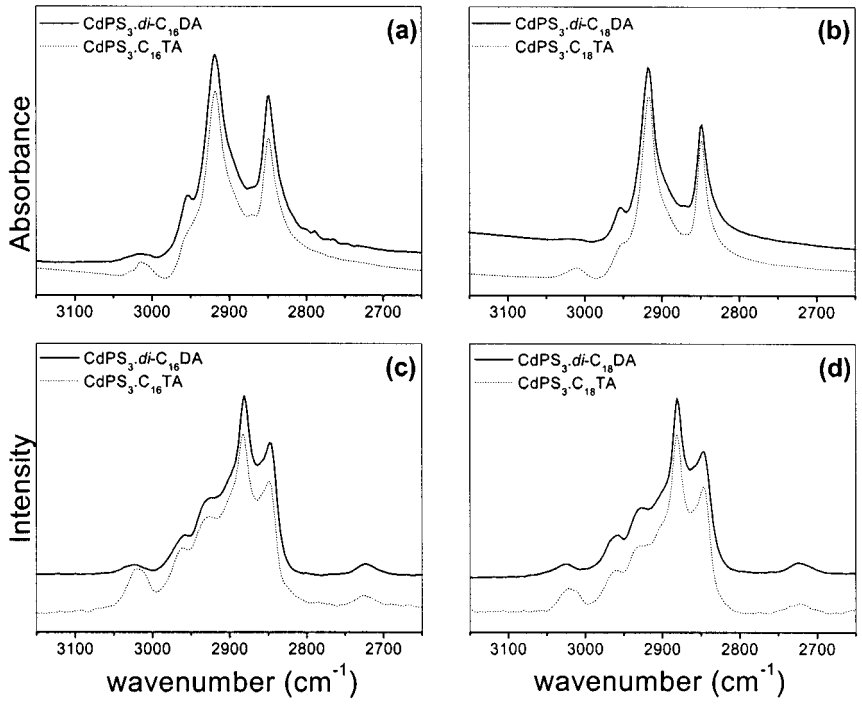


**Figure 3.** Infrared (a and b) and Raman (c and d) spectra in the C−H stretching region of the cationic lipid intercalate $CdPS_3$.*di*-$C_n$DA (solid line) together with the single chain analogues $CdPS_3$.$C_n$TA for $n = 16$ (a and c) and $n = 18$ (b and d).

respectively.[34] With increasing gauche conformers, as in the *n*-alkane melts, the line-width of these bands increases, and there is a shift to higher frequencies, typically 2856−2859 $cm^{-1}$ for the symmetric and 2924−2928 $cm^{-1}$ for the antisymmetric stretching mode.[35] The infrared spectrum in the methylene stretching region for the intercalated $CdPS_3$.*di*-$C_n$DA as well as the intercalated single chain $CdPS_3$.$C_n$TA are shown in Figure 3a,b. For the intercalated double chain compounds, the symmetric stretch appears at 2848 $cm^{-1}$, whereas the antisymmetric appears at 2918 $cm^{-1}$. The corresponding values for the single chain are 2850 and 2918 $cm^{-1}$. These methylene stretching mode frequencies indicate that a majority of the methylene units of the intercalated cationic lipids adopt a trans conformation.

The Raman spectrum of alkyl chain assemblies is dominated by two prominent bands, centered at 2880 and 2850 $cm^{-1}$, which are assigned to the methylene antisymmetric and symmetric stretching modes. The ratio of the intensities of the band at ∼2880 $cm^{-1}$ to that at ∼2850 $cm^{-1}$ ($I_{2880}/I_{2850}$) is known to be sensitive to both conformational disorder of the alkyl chains as well as their packing[37,38] and has been widely used to characterize alkyl chain assemblies.[3] The value of the intensity ratio, $I_{2880}/I_{2850}$, varies from ∼ 2 as in crystalline *n*-alkanes to ∼ 0.7 in the corresponding liquid-phase.[37] It has been shown that the intensity ratio $I_{2880}/I_{2850}$ is sensitive to both conformational order as well as lateral interactions arising from the packing arrangement. The FT-Raman spectrum of crystals of $CdPS_3$.*di*-$C_n$DA and $CdPS_3$.$C_n$TA in the C−H stretching region is shown in Figure 3c,d. Peaks due to the antisymmetric and symmetric methylene stretching modes are observed at 2882 and 2850 $cm^{-1}$. The intensity ratios $I_{2880}/I_{2850}$ for the cationic lipid intercalates $CdPS_3$.*di*-$C_n$DA are 1.38 and 1.44 for $n = 16$ and 18, respectively, whereas the ratios $I_{2880}/I_{2850}$ for the corresponding alkyl trimethylammonium intercalates $CdPS_3$.$C_n$TA are 1.34 and 1.36 for $n = 16$ and 18, respectively.

The methylene stretching modes in both the IR and Raman indicate a fair degree of trans conformational order in the alkyl chains of the intercalated cationic lipid. These modes are, however, not too sensitive to low concentrations of gauche disorder, and consequently, the spectra of the intercalated double chain cationic lipid show no significant difference from those of the intercalated single-chain compounds.

**Localized Methylene Wagging Modes (IR).** Methylene wagging modes in the IR spectrum of *n*-alkanes in the region 1300−1400 $cm^{-1}$ are known to exhibit peaks with characteristic frequencies for different conformational sequences.[39] These bands are specific to localized structures that contain a gauche bond. For example, a peak at 1341 $cm^{-1}$ indicates a penultimate bond oriented such that the terminal methyl group is in gauche conformation relative to the methylene group three carbon atoms away (end gauche, eg). A peak at 1354 $cm^{-1}$ is due to adjacent gauche bonds (*gg*), and a peak at 1368 $cm^{-1}$ arises from a gauche-trans-gauche′ ($g-t-g'$) sequence or a kink. Because these are localized modes, the area under the peak is proportional to the concentration of that particular sequence.[40] The methyl umbrella deformation band, which appears at 1377 $cm^{-1}$, is taken as an internal standard and the spectra in this region normalized with respect to this band.[41,42]

The infrared spectra in the localized methylene wagging modes region normalized with respect to the 1377 $cm^{-1}$ band for the intercalated cationic lipid are shown in Figure 4. The intensities of the 1368 $cm^{-1}$ band as well as the 1355 $cm^{-1}$ band corresponding to the $g-t-g'$ and *gg* conformations are almost absent, whereas the 1341 $cm^{-1}$ peak due to end gauche appears as a weak peak. In the intercalated single chain compounds, $CdPS_3$.$C_n$TA, the peak at 1365 $cm^{-1}$ because of the kink may be clearly seen, and the 1341 $cm^{-1}$ end-gauche defect band is relatively more intense than in the double chain intercalated, $CdPS_3$.*di*-$C_n$DA.

These results show that the methylene chains in the cationic lipid−$CdPS_3$ intercalates have fewer gauche defects as compared to the corresponding single chain alkyl trimethylammonium−$CdPS_3$ intercalates. This is a consequence of the increased density of the intercalated methylene chains in the former. Moreover, the gauche defects that are present occur at the end of the chain rather than in the middle. This is understandable because a gauche defect in the middle of the chain or close to

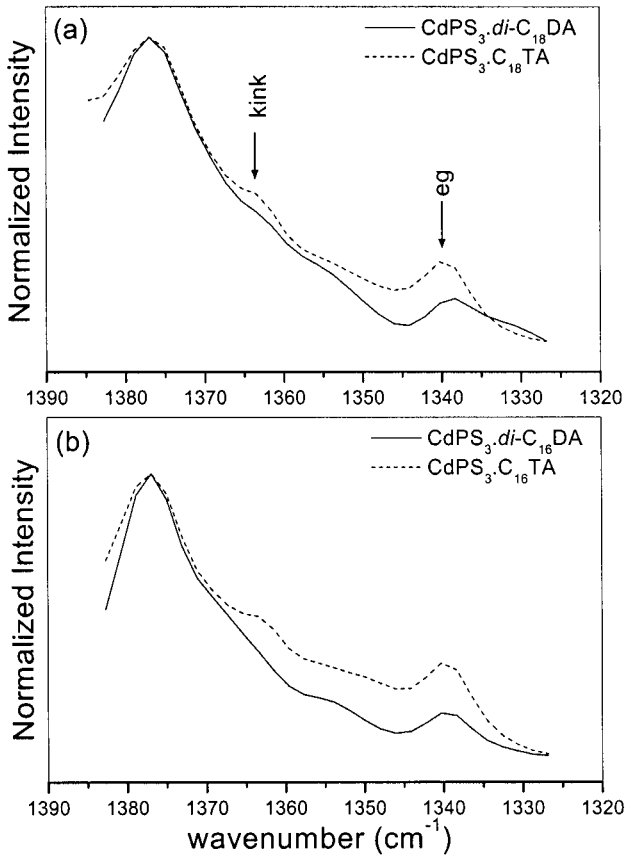


**Figure 4.** Infrared spectra in the region of localized methylene wagging modes of the intercalates $CdPS_3$.*di*-$C_n$DA (solid line) and $CdPS_3$.$C_n$-TA (dotted line) for $n = 18$ (a) and $n = 16$ (b).

the "head" of the grafted chain would lead to the chain requiring a large cross-sectional area.

The results so far indicate that concentration of gauche disorder in the intercalated cationic lipids is small, and consequently, we have examined the progression bands in the infrared spectra. These progressions arise exclusively from coupling of vibrational modes of methylene units in trans registry.[43−46] The number and spacing of these bands are diagnostic of all-trans chain length and hence can serve to distinguish completely ordered alkyl chains of different length that may be present.

**Progression Bands of the Methylene Chain.** Vibrational spectra of long chain molecules have been interpreted on the basis of vibrational modes of an infinite polymethylene chain.[47] Conformational order in alkyl chains causes a coupling of the methylene vibrational modes. Vibrational spectra of ordered alkyl chain systems have been analyzed based on dispersion curves by plotting the frequencies ($\nu$) as a function of the phase angle ($\phi$) between neighboring methylene units. For an infinite polymethylene chain, only vibrational modes at $\phi = 0$ or $\pi$ are infrared and/or Raman active. In the case of a finite chain, in addition to the $\phi = 0$ or $\pi$ mode, a series of bands, namely, progression bands, appear in the IR and/or Raman spectrum.[44] The progression bands are usually weak in intensity; however, it has been pointed out that end group substitution usually enhances the intensity of these progression bands as compared to the crystalline *n*-alkanes.[27] The progression bands appearing in the spectrum are analyzed by assigning a $k$ value after identifying the particular mode to which it belongs. When correctly assigned, a smooth dispersion curve results from a plot of $\nu_k$ vs $\phi_k$.[43,44] The progression bands arising from the $CH_2$ wagging ($\nu_3$), twisting−rocking ($\nu_7$), rocking−twisting ($\nu_8$),

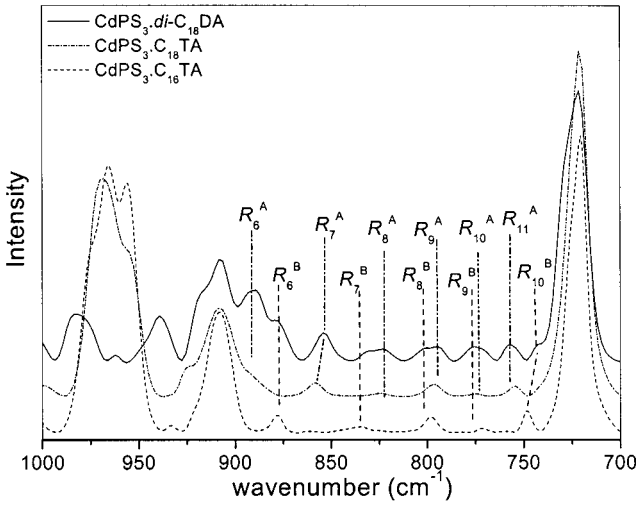


**Figure 5.** Infrared spectra in the methylene rocking-twisting ($R$) progression region of the intercalates $CdPS_3$.*di*-$C_{18}$DA (solid), $CdPS_3$.$C_{18}$-TA (dash−dot), and $CdPS_3$.$C_{16}$TA (dotted). Band assignments are given by the $k$ values (subscripts) and the progression series to which they belong by the label A ($N = 17$) and B ($N = 15$). $N$ is the number of coupled oscillators appearing in eq 1.

and C−C skeletal stretching ($\nu_4$) modes have been studied in detail for *n*-alkanes,[44] *n*-alcohols,[48] *n*-fatty acids,[49] and the CTA ion intercalated in $CdPS_3$.[50]

The allowed phase angles, $\phi_k$, for a finite chain can be obtained using the simple coupled oscillators approximation. For a chain having $N$ oscillators ($N$ methylene units in trans registry), $\phi_k$ is given by[43]

$$\phi_k = k\pi/(N+1)\ [k = 1,2,3,...N] \qquad (1)$$

It is clear that the spacing and number of progression bands depend on the number of methylene units in the trans registry. It may thus be seen that the progression bands could help to distinguish and estimate the relative concentrations of the TT and TG type ordered structures (Figure 1), because for the former both chains have identical $N$ coupled oscillators, whereas for the ordered TG structure the shorter chain has $N - 2$ coupled oscillators.

In the present study, we have analyzed the $CH_2$ rocking modes appearing in the 1000−700 $cm^{-1}$ region of the infrared spectrum because for these samples this region is relatively free from complications arising from overlapping bands. Attention is focused on the progression bands of the double-chain $CdPS_3$.*di*-$C_{18}$DA intercalate because direct comparison with the single chain $CdPS_3$.$C_{18}$TA and $CdPS_3$.$C_{16}$TA leads to less ambiguity in assignments.

The IR spectrum in the methylene rocking progression ($\nu_8$) region of the cationic lipid intercalate $CdPS_3$.*di*-$C_{18}$DA along with the alkylammonium intercalates $CdPS_3$.$C_{16}$TA and $CdPS_3$.$C_{18}$TA are shown in Figure 5. It can be seen from the spectrum of $CdPS_3$.*di*-$C_{18}$DA that the progression bands are relatively more intense as compared to either $CdPS_3$.$C_{18}$TA or CdP.$C_{16}$TA emphasizing the conclusion that the cationic lipid intercalates are conformationally more ordered with an enhanced all-trans conformational registry as compared to the single chain analogues.

The spectrum of $CdPS_3$.*di*-$C_{18}$DA shows a large number of bands in the 1000−700 $cm^{-1}$ region as compared to either $CdPS_3$.$C_{18}$TA or $CdPS_3$.$C_{16}$TA, indicating that there could be two sets of progression bands with differing spacings. This is corroborated by a comparison, which shows that many of the

**TABLE 2: Observed Rocking Band Progression Frequencies in $CdPS_3$.*di*-$C_{18}$TA, $CdPS_3$.$C_{18}$TA, and $CdPS_3$.$C_{16}$TA and Their Assignments**

| $CdPS_3$. *di*-$C_{18}$DA ($cm^{-1}$) | $CdPS_3$. $C_{16}$TA ($cm^{-1}$) | $CdPS_3$. $C_{18}$TA ($cm^{-1}$) | assignment |
|---|---|---|---|
| 721 (s) | 720 (s) | 721 (s) | |
| 743 (sh) | 748 (m) | | *R*-$17^A$, *R*-$15^B$ |
| 756 (m) | | 754 (m) | *R*-$10^B$ |
| 773 (m) | 771 (w) | 773 (w) | *R*-$11^A$ |
| 794 (m) | | 796 (m) | *R*-$10^A$, *R*-$9^B$ |
| 800 (sh) | 798 (m) | | *R*-$9^A$ |
| 823 (m) | | 825 (w) | *R*-$8^B$ |
| 831 (sh) | 835 (w) | | *R*-$8^A$ |
| 854 (s) | | 860 (m) | *R*-$7^B$ |
| 879 (sh) | 879 (m) | | *R*-$7^A$ |
| 890 (s) | | 891 (sh) | *R*-$6^B$ |
| 908 (s) | 908 (s) | 908 (s) | *R*-$6^A$ |
| 918 (sh) | | | $\nu_{C-N}^+$ |
| | | 925 (m) | |
| 939 (s) | 933 (w) | | *R*-$5^A$ |
| | | | *R*-$4^B$ |

features of the $CdPS_3$.*di*-$C_{18}$DA are present in the spectra of either $CdPS_3$.$C_{16}$TA or $CdPS_3$.$C_{18}$TA. By comparison with the spectra of the single chain, $CdPS_3$.$C_n$TA, the two different progression series could be identified. Features common to the intercalated *di*-$C_{18}$DA and single $C_{18}$TA chain could then be assigned $k$ values appropriate for a set of $N = 17$ (eq 1) coupled oscillators (labeled as A in Figure 5). The remaining bands appear at frequencies very similar to the progression bands of the intercalated CTA single chain and could therefore be assigned $k$ values appropriate for $N = 15$ (eq 1) coupled oscillators. The features corresponding to progressions for $N = 15$ are labeled as B in Figure 5. The observed band positions and the appropriate $k$ values for the $CdPS_3$.*di*-$C_{18}$DA along with $CdPS_3$.$C_{18}$TA and $CdPS_3$.$C_{16}$TA are given in Table 2. The progression bands indicate that in the cationic lipid intercalate, $CdPS_3$.*di*-$C_{18}$DA, two types of ordered alkyl chains are present, one in which the entire chain adopts an all-trans conformation ($N = 17$) and another with a gauche bond at the beginning of the chain ($N = 15$), similar to that observed in the crystalline state of these lipids. The dispersion curve ($\nu_k$ vs $\phi_k$) for the two progression series have been plotted in Figure 6 along with those for the intercalated single chains. It may be seen that both of the progression series show an identical dispersion and that all points lie on the calculated dispersion curve for an infinite polymethylene chain[43,47] (solid line in Figure 6).

The relative concentration of the TT and TG ordered chains can be estimated if the relative concentration of the A ($N = 17$) and B ($N = 15$) chains of the intercalated lipid can be determined. This can be done, following the procedure developed by Yan et al.,[27] from the ratio of the integrated intensities of selected bands corresponding to the two progression series for the A and B chains:

$$X_A/X_B = \kappa \sum I_{A_i}/I_{B_i} \qquad (2)$$

$X_A$ and $X_B$ are the molar concentrations of the A and B chains, and $I_{A_i}$ and $I_{B_i}$ are the integrated intensities of the rocking progression bands with $k = i$ of the A and B chains. The summation of the intensities is over a set of selected $k$ values. The proportionality constant, $\kappa$, relates the intensity ratio to the molar concentration ratio.

The proportionality constant was estimated from the spectrum of crystalline dioctadecyl dimethylammonium bromide (*di*-$C_{18}$-DAB) where it is known from X-ray crystallography that the concentration of A and B chains are identical ($X_A/X_B = 1$).[24,25] The spectrum of *di*-$C_{18}$DAB is shown in Figure 7. Two sets of progression bands are observed, and from a comparison of the rocking mode progression bands of the single chain CTAB and ODTAB (Figure 7), bands associated with the two progressions can be identified. In Figure 7, the rocking bands have been labeled by their $k$ values and the progression series to which they belong, A for $N = 17$ and B for $N = 15$ ($N$ is the number

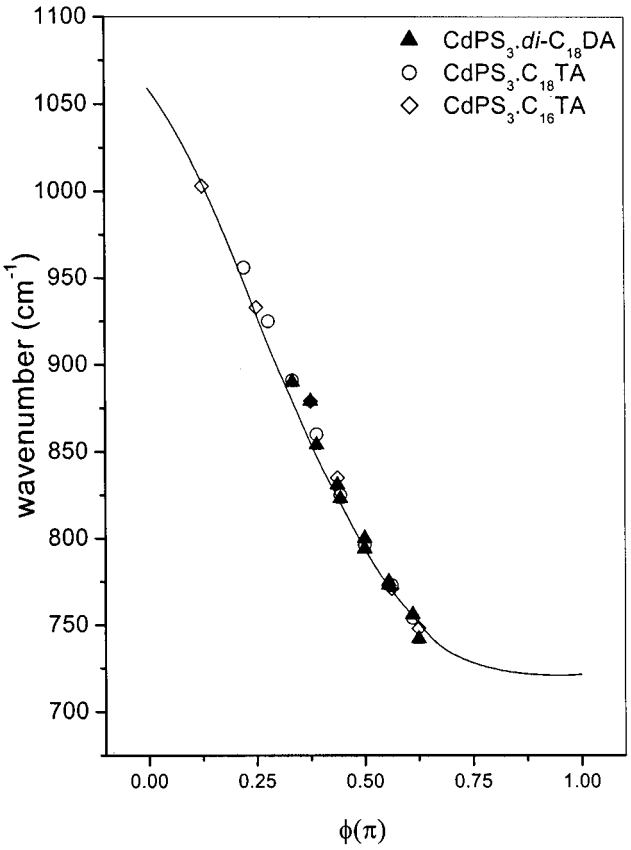


**Figure 6.** Dispersion of the methylene rocking-twisting progression for the intercalates $CdPS_3$.*di*-$C_{18}$DA (▲), $CdPS_3$.$C_{18}$TA (○), and $CdPS_3$.$C_{16}$TA (◇). The solid line is the calculated dispersion curve for an infinite polymethylene chain.[43,47]

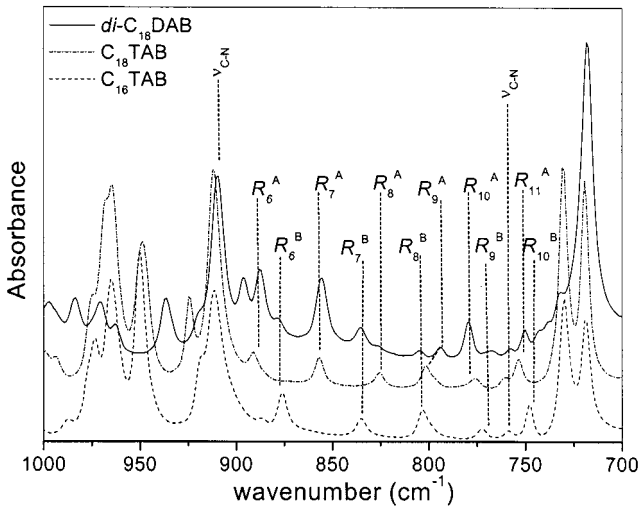


**Figure 7.** Infrared spectrum of crystalline *di*-$C_{18}$DAB (solid line) in the methylene rocking-twisting (*R*) progression region along with the single chain analogues ODTAB (dash−dot line) and CTAB (dotted line). The assignments of the progression bands are given by their $k$ value (subscripts), and the progression series to which they belong are given by the label A or B.

**TABLE 3: Fraction of Intercalated Lipid Molecules with TT and TG Ordered Structures at Different Temperatures in $CdPS_3$.*di*-$C_{18}$DA along with the Parameters Used in the Estimation**

| | bands selected | | temp | | $\Sigma(I_A)/\Sigma(I_B)$ | $X_A/X_B$ | fraction of molecules with |
|---|---|---|---|---|---|---|---|
| | A | B | (K) | $\kappa$ | (observed) | (estimated) | TG(TT) conformation |
| crystalline | 794 | 804 | 298 | | 0.450 | 1 | 1(0) |
| *di*-$C_{18}$DAB | 823 | 831 | | | | | |
| intercalate | 796 | 803 | 75 | 2.22 | 0.988 | 2.193 | 0.63 (0.37) |
| $CdPS_3$.*di*-$C_{18}$DA | 823 | 831 | 150 | | 1.089 | 2.418 | 0.59 (0.41) |
| | | | 200 | | 1.056 | 2.344 | 0.60 (0.40) |
| | | | 250 | | 0.958 | 2.127 | 0.64 (0.36) |
| | | | 300 | | 1.089 | 2.418 | 0.59 (0.41) |

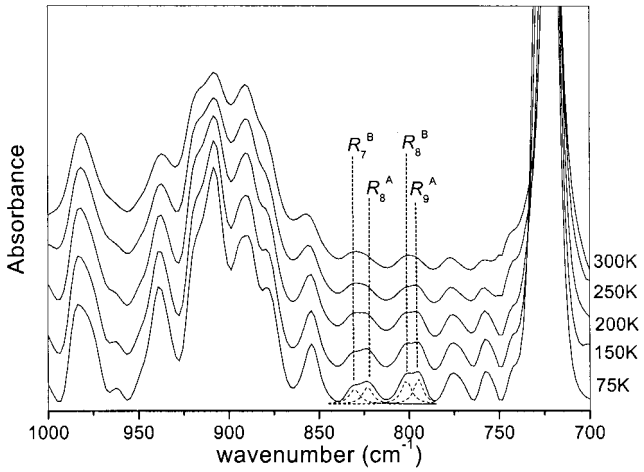


**Figure 8.** Temperature dependence of the infrared spectrum of the cationic lipid intercalate $CdPS_3$.*di*-$C_{18}$DA in the methylene rocking-twisting progression region. Dotted lines are the individual Lorentzian components of the fit to the observed bands in the 75 K spectrum used in the determination of the fraction of TT and TG ordered structures.

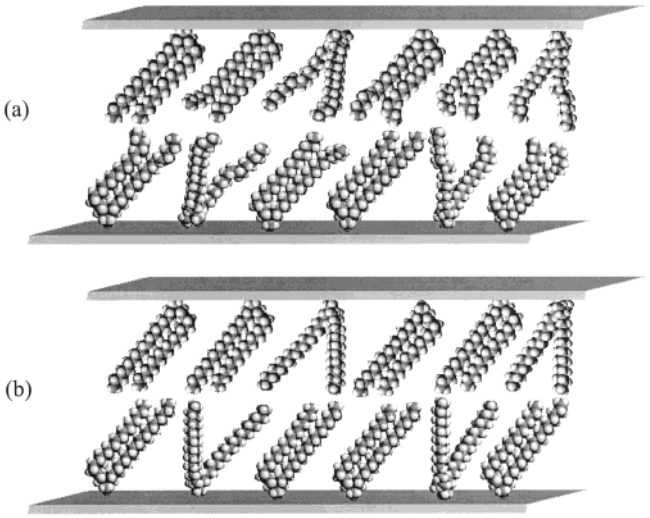


**Figure 9.** Cartoon representation of conformation of the intercalated cationic lipids in $CdPS_3$.*di*-$C_{18}$DA at two different temperatures (a) 300 and (b) 75K. The overall conformational disorder in the intercalate decreases as the temperature is decreased, whereas the concentrations of the TG and TT ordered structures remain unaltered.

of coupled oscillators appearing in eq 1). The bands selected for calculating the proportionality constant are the bands with $k$ values of 8 and 9 for the A ($N = 17$) and 7 and 8 for the B ($N = 15$) chains. Because of the overlap of bands, the individual integrated peak intensities were obtained by fitting the contour by a sum of two Lorentzians. The proportionality constant so determined is 2.22 (Table 3).

The molar concentrations of the A ($N = 17$) and B ($N = 15$) chains for the intercalated cationic lipid ($CdPS_3$.*di*-$C_{18}$DA), $X_A$ and $X_B$, were estimated using eq 2. The bands selected had the same $k$ value as those bands used for estimating the proportionality constant $\kappa$. Overlap of the bands of the A and B chains required that the band contours be fitted with two Lorentzians to obtain the individual peak intensities. A typical fit is shown in Figure 8, and the results are summarized in Table 3. From the ratio of the concentration of the A ($N = 17$) and B ($N = 15$) chains, the relative concentrations of the TT and TG ordered structures were determined and these are $\sim 0.4$ and $\sim 0.6$, respectively.

We have also measured the temperature variation of the relative concentrations of the intercalated TT and TG chains. The rocking mode progression bands of the intercalate $CdPS_3$.*di*-$C_{18}$DA at different temperatures are shown in Figure 8. The intensities of the progression bands, as expected, increases with decreasing temperature because of increased conformational order at low temperatures. At all temperatures, bands due to the progression series corresponding to $N = 17$ and 15 coupled oscillators are seen and their relative concentrations are determined by the method described above. The results of the analysis are given in Table 3. Although the overall intensity of the all-trans ordered chains increases with decreasing temperature, the relative concentrations of the TT and TG ordered structures show no change with temperature.

The large increase in the concentration of TT ordered structures as compared to the crystalline bromide salt (where TT structures are absent) may be understood on the basis of the molecular volume available for the cationic lipid in the intercalated state. It may be seen from Figure 1 that the TT ordered structure of the lipid occupies a much larger volume as compared to the TG structure. In the crystalline state of these cationic lipids, an efficient packing arrangement requires that all alkyl chains exclusively adopt the TG ordered structure. Whereas for the intercalated cationic lipid, no such constraint exists. Moreover the grafting density in the galleries is such that the interlamellar volume can accommodate a fraction of the intercalated lipid cations with the TT ordered structure (Figure 9). The fact that the ratio of TT to TG structures remains unchanged with temperature is also not surprising because changes in conformational order in lipids with temperature usually occurs at the chain end[51] rather than close to the head. Interconversion of TT and TG structures would however require changes in conformation of the $CH_2-CH_2$ bond adjacent to the head.

**Supporting Information Available:** Figure 1 Infrared spectra in the region of 3200−700 cm$^{-1}$ of the intercalated cationic lipids $CdPS_3$.*di*-$C_n$DA and the corresponding single chain analogues $CdPS_3$.$C_n$TA. Figure 2 Raman spectra in the region of 3200−700 cm$^{-1}$ of the intercalated cationic lipids $CdPS_3$.*di*-$C_n$DA and the corresponding single chain analogues

$CdPS_3.C_nTA$. This material is available free of charge via the Internet at http://pubs.acs.org.

## References and Notes


(1) Sackmann, E. *Science* **1996**, *271*, 43.
(2) Boxer, S. G. *Curr. Opin. Chem. Biol.* **2000**, *4*, 704.
(3) Wallach, D. F. H.; Verma, S. P.; Fookson, J. *Biochim. Biophys. Acta* **1979**, *559*, 153.
(4) Levin, I. L. In *Advances in Infrared and Raman Spectroscopy*; Clark, R. J. H., Hester, R. E., Eds.; Wiley-Heyden: New York, 1984; Vol. 11, p 1−48.
(5) Mendelsohn, R.; Senak, L. *Biomolecular Spectroscopy, Part A*; Clark, R. J. H., Hester, R. E., Eds.; John Wiely: New York, 1993; pp 339−380.
(6) Kunitake, T.; Okahata, Y. *J. Am. Chem. Soc.* **1977**, *99*, 3860.
(7) Kawai, T.; Umemura, J.; Takenaka, T.; Kodama, M.; Ogawa, Y.; Seki, S. *Langmuir* **1986**, *2*, 739.
(8) Shimada, I.; Ishida, A.; Ishitani, A.; Kunitake, T. *J. Colloid Interface Sci.* **1987**, *120*, 523.
(9) Bhattacharya, S.; Haldar, J. *Biochim. Biophys. Acta* **1996**, *1283*, 21.
(10) Lagaly, G. *Angew. Chem., Int. Ed. Eng.* **1976**, *15*, 575.
(11) Lagaly, G. *Solid State Ionics* **1986**, *22*, 43.
(12) Ogawa, M.; Kuroda, K. *Bull. Chem. Soc. Jpn.* **1997**, *70*, 2593.
(13) Vaia, R, A.; Teukolsky, R, K.; Giannelis, E, P. *Chem. Mater.* **1996**, *6*, 1017.
(14) Matsuo, Y.; Hatase, K.; Sugie, Y. *Chem. Commun.* **1999**, 43.
(15) Yang, J. H.; Han, Y. S.; Choy, J. H.; Tateyama, H. *J. Mater. Chem.* **2001**, *11*, 1305.
(16) LeBaron, P. C.; Wang, Z.; Pinnavaia, T. J. *Appl. Clay Sci.* **1999**, *15*, 11.
(17) Alexandre, M.; Dubois, P. *Mater. Sci. Eng.* **2000**, *28*, 1.
(18) Kerr, T. A.; Leroux, F.; Nazar, L. F. *Chem. Mater.* **1998**, *10*, 2588.
(19) Wolfe, T, A.; Demirel, T.; Baumann, E, R. *Clays Clay Miner.* **1985**, *33*, 301.
(20) Mortland, M. M.; Shaobai, S.; Boyd, S, A. *Clays Clay Miner.* **1986**, *34*, 581.
(21) Venkataraman, N. V.; Vasudevan, S. *J. Phys. Chem. B* **2001**, *105*, 1805.
(22) Ouvrard, G.; Brec, R.; Rouxel, J. *Mater. Res. Bull.* **1985**, *20*, 1181.
(23) Brec, R. *Solid State Ionics* **1986**, *22*, 3.
(24) Okuyama, K.; Soboi, Y.; Iijima, N.; Hirabayashi, K.; Kunitake, T.; Kajiyama, T. *Bull. Chem. Soc. Jpn.* **1988**, 1485.
(25) Okuyama, K.; Iijima, N.; Hirabayashi, K.; Kunitake, T.; Kajiyama, T. *Bull. Chem. Soc. Jpn.* **1988**, 2337.
(26) Pearson, R. H.; Pascher, I. *Nature* **1979**, *281*, 499.
(27) Yan, W. H.; Strauss, H. L.; Snyder, R. G. *J. Phys. Chem. B* **2000**, *104*, 4229.
(28) Klingen, V. W.; Ott, R.; Hahn, H. *Z. Anorg. Allg. Chem.* **1973**, *396*, 271.
(29) Clement, R. *J. Chem. Soc., Chem. Commun.* **1980**, 647.
(30) Clement, R.; Garnier, O.; Jegoudez, J. *Inorg. Chem.* **1986**, *25*, 1404.
(31) Jeevanandam, P.; Vasudevan, S. *Solid State Ionics* **1997**, *104*, 45.
(32) Venkataraman, N. V.; Vasudevan, S. *J. Phys. Chem. B* **2000**, *104*, 11179.
(33) Snyder, R. G. *J. Mol. Spectrosc.* **1964**, *7*, 116.
(34) MacPhail, R. A.; Strauss, H. L.; Snyder, R. G.; Elliger, C. A. *J. Phys. Chem.* **1984**, *88*, 334.
(35) Snyder, R. G.; Strauss, H. L.; Elliger, C. A. *J. Phys. Chem.* **1982**, *86*, 5145.
(36) Casal, H. L.; Mantsch, H. H.; Cameron, D. G.; Snyder, R. G. *J. Chem. Phys.* **1982**, *77*, 2825.
(37) Snyder, R. G.; Hsu, S. L.; Krimm, S. *Spectrochim. Acta* **1978**, *34*, 395.
(38) Brown, K. G.; Bicknell-Brown, E.; Ladjadj. *J. Phys. Chem.* **1987**, *91*, 3436.
(39) Snyder, R. G. *J. Chem. Phys.* **1967**, *47*, 1316.
(40) Snyder, R. G. *Macromolecules* **1990**, *23*, 2081.
(41) Holler, F.; Callis, J. B. *J. Phys. Chem.* **1989**, *93*, 2053.
(42) Casal, H. L.; McElhaney, R, N. *Biochemisty* **1990**, *29*, 5423.
(43) Snyder, R. G. *J. Mol. Spectrosc.* **1960**, *4*, 411.
(44) Snyder, R. G.; Schachtschnelder, J. H. *Spectrochim. Acta* **1963**, *19*, 85.
(45) Yano, J.; Kaneko, F.; Kobayashi, M.; Sato, K. *J. Phys. Chem. B* **1997**, *101*, 8112.
(46) Senak, L.; Moore, D.; Mendelsohn, R. *J. Phys. Chem.* **1992**, *96*, 2749.
(47) Tasumi, M.; Shimonauchi, T.; Miyazwa, Y. *J. Mol. Spectrosc.* **1962**, *9*, 261.
(48) Tasumi, M.; Shimaanouchi, T.; Watanabe, A.; Goto, R. *Spectrochim. Acta* **1964**, *20*, 629.
(49) Kobayashi, M.; Kaneko, F.; Sato, K.; Suzuki, M. *J. Phys. Chem.* **1989**, *93*, 485.
(50) Venkataraman, N. V.; Vasudevan, S. *J. Phys. Chem. B* **2001**, *105*, 7639.
(51) Maroncelli, M.; Strauss, H. L.; Snyder, R. G. *J. Chem. Phys.* **1985**, *82*, 2811.